The interaction of cobalt species with alumina on Co/Al2O3 catalysts prepared by atomic layer deposition

ARTICLE *in* APPLIED CATALYSIS A GENERAL · JUNE 2009

Impact Factor: 3.94 · DOI: 10.1016/j.apcata.2009.03.020

4 AUTHORS, INCLUDING:

Leif Backman
Finnish Meteorological Institute
41 PUBLICATIONS **528** CITATIONS

Applied Catalysis A: General 360 (2009) 183–191

Contents lists available at ScienceDirect

Applied Catalysis A: General

journal homepage: www.elsevier.com/locate/apcata

The interaction of cobalt species with alumina on Co/Al_2O_3 catalysts prepared by atomic layer deposition

L.B. Backman [a,*], A. Rautiainen [b], M. Lindblad [c], A.O.I. Krause [a]

[a] Helsinki University of Technology, Faculty of Chemistry and Materials Science, P.O. Box 6100, FI-02015 TKK, Finland
[b] Neste Oil Corp., Naantali Refinery, FI-21100 Naantali, Finland
[c] Neste Oil Corp., P.O. Box 310, FI-06101 Porvoo, Finland

ARTICLE INFO

Article history:
Received 5 December 2008
Received in revised form 2 March 2009
Accepted 17 March 2009
Available online 25 March 2009

Keywords:
Cobalt catalysts (supported)
Alumina
Atomic layer deposition
ALD
Reducibility
Dispersion
Calcination
Toluene hydrogenation

ABSTRACT

Alumina supported cobalt catalysts were prepared by atomic layer deposition (ALD) of cobalt acetylacetonate precursors ($Co(acac)_2$ and $Co(acac)_3$). The main modes of interaction between the acetylacetonate precursors and the support were found to be the exchange reaction between the alumina OH-groups and the acac-ligands of the precursor and dissociative adsorption on coordinatively unsaturated Al^{3+} sites. The amount of precursor that could adsorb on the support was determined by steric hindrance. Samples were prepared using 1–5 reaction cycles, i.e. subsequent precursor addition ($Co(acac)_2$) and calcination, resulting in catalysts containing ca. 3–10 wt.% Co. Samples were also prepared where the last calcination step was omitted, i.e. uncalcined catalysts. Calcination at 450 °C decreased the reducibility of the $Co(acac)_2/Al_2O_3$ catalysts due to formation of a cobalt oxide phase strongly interacting with the support and aluminate type surface species. The reducibility increased with metal loading on both calcined and uncalcined catalysts; however the reducibility of the calcined catalysts remained lower than of the uncalcined ones. The dispersion was found to be lower on the calcined catalysts. The cobalt particle sizes on the calcined samples was ca. 8 nm and on the uncalcined 4–5 nm, for cobalt loadings of ca. 6–10 wt.%. Catalytic activity was tested by gas phase hydrogenation of toluene in temperature programmed mode (30–150 °C).

1. Introduction

The interaction between the active component and the support greatly influences the properties of a supported catalyst. In general, a weaker interaction gives larger particles and a higher reducibility, and respectively, a stronger interaction smaller particles and lower reducibility (e.g. [1,2]). All factors that affect the interaction between the supported species and the support during the preparation will therefore also affect the particle size and the reducibility of the catalyst. Typically the activity of a hydrotreating catalyst is dependent on the available metal surface area, i.e. for a given loading the activity increases with dispersion. However, the dispersion of the active species can also affect the specific activity and selectivity of a reaction, e.g. for particle sizes below 6 nm the specific activity and C^{5+} selectivity was found to decrease with particle size in the Fischer–Tropsch reaction [3]. Also the deactivation of cobalt catalysts in CO hydrogenation has been reported to depend on the particle size. The deactivation possibly involves reoxidation of highly dispersed cobalt by water [4–6].

The support material is an important factor in determining the dispersion and reducibility of cobalt. Usually porous oxides such as Al_2O_3, SiO_2 and TiO_2 are used to disperse the active species. In general the formation of poorly reducible cobalt surface compounds has been found to be more limited on silica than on alumina [1,7,8]. However, it is known that well dispersed silica supported cobalt in some conditions can form significant amounts of poorly reducible silicate type compounds [9–13]. The degree of reduction has been found to increase with cobalt crystallite size for particles up to ca. 15 nm on Al_2O_3, SiO_2 and TiO_2, due to decreasing metal support interaction [1]. Alumina supported cobalt readily forms surface compounds that only reduce at elevated temperatures (e.g. [1,7,8,14,15]). Temperature programmed reduction (TPR) has frequently been used as a method for studying the species formed on Co/Al_2O_3 catalysts. However, the interpretation of the TPR profiles varies. The species reducing at temperatures above 400–500 °C has most recently been interpreted to be either CoO interacting with the support [16] or a mixed cobalt aluminate type compound deficient in Co [15]. The relative amounts of the various species depend on the cobalt content and the conditions during the preparation. Direct reduction of the precursor has been

* Corresponding author. Present address: Finnish Meteorological Institute, Climate Change, Erik Palmenin aukio 1, P.O. Box 503, FI-00101 Helsinki, Finland. Tel.: +358 9 1929 4179; fax: +358 9 1929 3146.
E-mail addresses: Leif.Backman@fmi.fi, leif.backman@helsinki.fi (L.B. Backman).

0926-860X/$ – see front matter © 2009 Elsevier B.V. All rights reserved.
doi:10.1016/j.apcata.2009.03.020

found to increase the reducibility of Co/Al_2O_3 catalysts [2,14,17]. The activation (reduction) conditions also influence the dispersion and reducibility of the catalysts. Water vapor added during reduction with hydrogen enhances formation of aluminate type species [15], while addition of CO has been found to increase both the degree of reduction and dispersion [18]. The addition of promoters such as Re [5,19], Ru [1,2,15] or Pt [1,16,20] has been shown to enhance the reducibility and also dispersion.

In addition to the materials and the route to produce metallic cobalt, the final dispersion of cobalt also depends on the distribution of the precursor. For example by changing the pH of the impregnation solution the interaction between the cobalt nitrate precursor and the support was altered and therefore also the particle size changed [21]. By adding citric acid to the cobalt nitrate impregnating solution 'fully' dispersed hard to reduce (>600 °C) Co/Al_2O_3 sample was obtained [2].

Atomic layer deposition (ALD, also known as atomic layer epitaxy, ALE), is a preparation method based on saturating gas–solid reactions between precursor and support (e.g. [22]). The properties of both silica [12–14,22–24] and alumina [14] supported catalysts prepared by chemisorption of $Co(acac)_2$ or $Co(acac)_3$ by ALD have been reported previously. These studies showed that supported catalysts produced by deposition of cobalt acetylacetonate precursors through the gas phase gave well dispersed catalysts with strong precursor–support interaction. The activation of these catalysts required high reduction temperatures. The properties were found to depend strongly on the calcination [12,14].

In this paper, we have studied Co/Al_2O_3 catalysts prepared by addition of cobalt acetylacetonate precursors via the gas phase. The aim of this work was to study the chemisorption of cobalt acetylacetonates on alumina, the interaction of cobalt species with alumina and the effect of the interaction on the properties of the catalysts, e.g. reducibility and dispersion. The chemisorption mechanisms of $Co(acac)_2$ and $Co(acac)_3$ from the gas phase on silica have been reported previously [23,24]. In an earlier work the dispersion and reducibility of silica and alumina supported ALD samples were compared [14]. However, the interaction of cobalt acetylacetonate precursors and alumina ALD has not been reported earlier. A more detailed study of the interaction of the precursor with the support and the catalyst properties are presented. The activity of the catalysts was also tested for gas phase toluene hydrogenation. The experiments were done in a transient mode.

2. Experimental

2.1. Catalyst preparation

Alumina supported cobalt catalysts were prepared by chemisorption of cobalt acetylacetonate precursors via the gas phase by atomic layer deposition (ALD). The catalyst preparation by ALD (e.g. [22]) consisted of the following steps: (a) preheating of the support, (b) chemisorption of the gaseous cobalt precursor up to surface saturation, and (c) removal of the remaining ligands by calcination in synthetic air. The steps (b) and (c) were repeated up to five times to increase the cobalt content.

The alumina support (Akzo 000-1.5E alumina, crushed and sieved to a particle size of 0.15–0.35 mm) was precalcined under air in a muffle furnace at 600 °C/16 h or 875 °C/6 h. The precalcination temperature is indicated in the text as follows, e.g. 600-Al_2O_3. The support was further heated under flowing nitrogen in the ALD reactor at 300 °C/3 h or 450 °C/3 h, respectively.

The catalyst samples were prepared in a flow-type ALD reactor at about 10 kPa with nitrogen (AGA) as carrier gas. The cobalt(II)acetylacetonate ($Co(acac)_2$, Aldrich, 97%) was dried before use while the cobalt(III)acetylacetonate ($Co(acac)_3$, Merck, >98%), was used as received. The alumina support (5 g) was kept in a fixed bed (180 °C) and the precursors were evaporated at 170 and 180 °C, respectively, and passed through the support with nitrogen as carrier gas. The amount of vaporised precursors was kept high enough to ensure saturation of the surface. The precursor addition was followed by a nitrogen purge at the same temperature. After precursor chemisorption, the system was either cooled down in nitrogen or the acac-ligands were removed with synthetic air (AGA) at 450 °C for 4 h. Two sets of catalysts were prepared: one where the samples were calcined after each deposition step, referred to in the text as 'calcined catalysts', and another where the calcination after the last deposition step was omitted, 'uncalcined catalysts'. A H(acac)/600-Al_2O_3 sample, used as an IR reference, was prepared by adsorption of H(acac) at 200 °C.

2.2. Cobalt and carbon analysis

The cobalt concentration of the catalysts was measured with atomic absorption spectrometry (AAS, Varian SpectrAA-600), inductively coupled plasma mass spectrometry (ICP-MS, VGA Plasma Quad PQ2 Plus) or instrumental neutron activation analysis (INAA, Triga Mk II). The samples for the AAS measurements were prepared by dissolving the catalysts in a mixture of hydrochloric, nitric and hydrofluoric acid. The samples for the ICP-MS measurements were dissolved in nitric acid. A LECO CR 12 carbon analyser was used to measure the amount of carbon.

2.3. Drifts

The species formed on the alumina after chemisorption of the cobalt acetylacetonate precursors were studied by diffuse reflectance IR Fourier transform spectroscopy (DRIFTS, ATI Mattson Galaxy Series 6020 FTIR-spectrometer). The spectra were recorded over the wavenumber range 4000–600 cm^{-1} with a resolution of 2 cm^{-1}. The samples were ground to a fine powder and diluted with KBr. The DRIFT spectra were measured of uncalcined one-cycle samples. Both precursor ($Co(acac)_2$, $Co(acac)_3$) and support pretreatment temperature (600, 875 °C) was varied. The spectra of the precursors and a H(acac)/600-Al_2O_3 sample were measured for reference. The DRIFT spectra were plotted as reflectance vs. wavenumber.

2.4. Physisorption, chemisorption and oxygen titration

The nitrogen physisorption, hydrogen and CO chemisorption and oxygen titration measurements were all done with a Coulter OMNISORP 100CX. The surface area (BET) and pore volume were measured by nitrogen physisorption, at the temperature of liquid nitrogen. The static volumetric method was used. Prior to measurement the samples were outgassed at 90 °C for 1 h followed by outgassing at 300 °C, down to less than 10^{-5} mbar pressure for 3 h.

The H_2-chemisorption capacity was determined by static volumetric measurements. The samples were purged with helium at 150 °C for 30 min. Thereafter, the temperature was increased in vacuum by 10 °C/min to the reduction temperature. The catalysts were reduced in flowing hydrogen at 450–650 °C for 7 h followed by outgassing for 60 min at the reduction temperature before cooling the sample to the measurement temperature. Evacuation at the reduction temperature has been found to be the most advantageous for H_2-chemisorption on cobalt [25]. The H_2-chemisorption was measured at 100 °C due to activated chemisorption of hydrogen on supported cobalt (e.g. [14,25,26]). The chemisorption of carbon monoxide was measured at 30 °C. Both total and reversible isotherms were measured. The total hydrogen

uptake was used together with the degree of reduction obtained from O_2-titration to estimate the dispersion and particle size of metallic cobalt. The chemisorption procedure and formulas are described in detail in Ref. [27].

The degree of reduction was measured by O_2-titration [26]. Prior to the O_2-titration the samples were reduced *in situ* in flowing hydrogen at 450–650 °C for 7 h and outgassed at the reduction temperature for 60 min. The oxygen consumption was measured at 400 °C by the static volumetric method with a 20 vol.% O_2/He gas mixture. Metallic cobalt was assumed to oxidise fully to Co_3O_4 at these conditions.

2.5. Temperature programmed reduction

Temperature programmed reduction (TPR) measurements were performed with an Altamira Instruments AMI-100 catalyst characterisation system. The catalyst samples (50 mg) were purged with argon at 450 °C for 30 min and cooled to 50 °C. The samples were then heated from 50 to 700 °C at a rate of 10 °C/min while flowing a 11.2 vol.% H_2/Ar mixture (30 cm^3/min) through the sample. The consumption of hydrogen was monitored by a thermal conductivity detector (TCD). In some of the measurements, the outlet gas stream was also analysed with a mass spectrometer (Balzers MSC-200 Thermocube), equipped with a secondary electron multiplier (channeltron) detector.

2.6. Temperature programmed reaction–hydrogenation of toluene

Some of the catalysts were tested for gas phase toluene hydrogenation. The reaction runs were performed by increasing the reaction temperature from 30 to 150 °C at a rate of 1 °C/min. The product stream was analysed online with a mass spectrometer, the same as used in the TPR measurements. An Altamira Instruments AMI-100 catalyst characterisation system was used as reactor. The catalyst (25 mg) was crushed and sieved to a particle size of 0.1–0.2 mm and packed in a quartz u-tube. The catalysts were reduced *in situ* in flowing hydrogen.

The feed consisted of an 11.2 vol.% H_2/Ar mixture (30 cm^3/min) that was saturated with toluene by bubbling it through a flask kept at 0 °C in an ice bath. This resulted in a feed (0.08 mol/h) containing 0.89 vol.% toluene, 11.1 vol.% hydrogen and 88.0 vol.% argon. The following mass numbers were used in the mass spectrometer analysis: 98, 91, 83 and 55 for methylcyclohexane, 92 and 91 for toluene, 40 for argon and 2 for hydrogen. A linear relationship between concentration and ion current was verified by measuring different concentrations of toluene, methylcyclohexane and hydrogen in argon.

3. Results and discussion

3.1. Chemisorption of the precursors

Prior to chemisorption of the precursors the alumina support was calcined at 600 or 875 °C. Pretreatment of the alumina support at 600 °C gave a surface area of 180 m^2/g and a pore volume of 0.50 cm^3/g, which corresponds to an average pore diameter of 11 nm. The corresponding properties after pretreatment at 875 °C were 133 m^2/g, 0.48 cm^3/g and 14 nm. The OH group concentration (^{1}H MAS NMR) on the 600-Al_2O_3 sample has been measured to 2 OH/nm^2 [28] and the concentration on the 875-Al_2O_3 was 0.8 OH/nm^2.

The cobalt content of the Co/Al_2O_3 catalysts prepared by ALD using $Co(acac)_2$ or $Co(acac)_3$ are given in Table 1. One reaction cycle of $Co(acac)_2$ gave 3.8 wt.% Co on alumina precalcined at 600 °C and 2.6 wt.% on alumina precalcined at 875 °C. A similar trend was observed for one reaction cycle of $Co(acac)_3$, 2.7 and 1.8 wt.%, respectively. However, the decrease in cobalt content given per surface area was less prominent, with a decrease from 2.3 to 2.1 Co/nm^2 for $Co(acac)_2$ and from 1.7 to 1.5 Co/nm^2 for $Co(acac)_3$. This clearly shows that the cobalt content correlated with the surface area of the support.

The amount of carbon in relation to cobalt can give an indication about the type of surface species present on the uncalcined samples. The C/Co ratio was 5.6 for $Co(acac)_2$ on 600-Al_2O_3 and 6.6 on 875–Al_2O_3 and for $Co(acac)_3$ the ratios were 9.6 and 11.7, respectively (Table 1). One acac-ligand contains five carbon atoms, assuming that the ligands remain intact on the samples these ratios would give about on 1–1.5 ligands per Co for $Co(acac)_2$ and around two ligands per Co for $Co(acac)_3$. The C/Co ratio increased with support pretreatment temperature, which indicated a change in the precursor support interaction.

DRIFTS measurements can be used to support or discard the assumptions made based on the elemental analysis. The DRIFT spectra of the precursors, $Co(acac)_2$ and $Co(acac)_3$, showed absorption bands of the acac-ligands similar to reported values [29–33]. The characteristic lines of the ligand methyl groups at 3200–2800 cm^{-1} were seen in the spectra of the $Co(acac)_2$/875-Al_2O_3, $Co(acac)_3$/875-Al_2O_3 and H(acac)/600-Al_2O_3 samples with only small variations in the relative intensities (not shown). In the spectra of the $Co(acac)_2$/875-Al_2O_3 the stretching vibrations of the conjugated chelate ring system [ν(C=C) + ν(C=O)] were seen at 1594 and 1521 cm^{-1} (Fig. 1, line a). These values agree well with the wavenumbers obtained for the bulk precursor both measured and reported [30–33] values, 1601–1588 and 1521–1513 cm^{-1}. The corresponding bands for the $Co(acac)_3$/875-Al_2O_3 were observed at

Table 1
The cobalt and carbon content and ratios of the catalysts prepared using $Co(acac)_2$ and $Co(acac)_3$.

Support pretreatment	Cycles	Co (wt.%)	Co (nm^{-2})	C (wt.%)	Ligand (nm^{-2})	C/Co last cycle	ligand/Co last cycle
$Co(acac)_2$ uncalcined							
600 °C/16 h	1	3.8[a]	2.3	4.4	2.6	5.6	1.1
875 °C/6 h	1	2.6[b]	2.1	3.5	2.8	6.6	1.5
875 °C/6 h	3	6.3[b]	5.4	3.4	2.8	9.0	1.8
875 °C/6 h	5	9.8[b]	8.6	3.3	2.9	9.4	1.9
$Co(acac)_2$ calcined							
875 °C/6 h	1	3.0[a]	2.3				
875 °C/6 h	3	6.4[b]	5.2				
875 °C/6 h	5	9.2[b]	7.8				
$Co(acac)_3$ uncalcined							
600 °C/16 h	1	2.7[c]	1.7	5.4	3.2	9.6	1.9
875 °C/6 h	1	1.8[c]	1.5	4.4	3.5	11.7	2.3

[a] Analysis by ICP-MS.
[b] Analysis by INAA.
[c] Analysis by AAS.

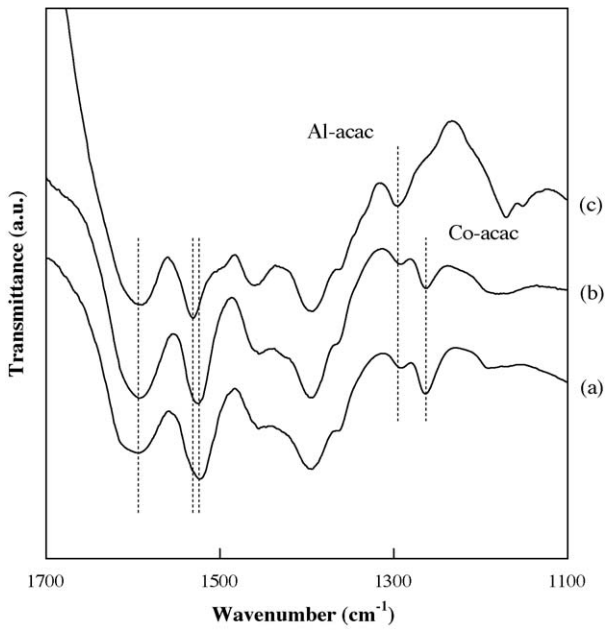

Fig. 1. IR spectrum of (a) $Co(acac)_2$/875-Al_2O_3, (b) $Co(acac)_3$/875-Al_2O_3 and (c) H(acac)/600-Al_2O_3.

1593 and 1525 cm^{-1} (Fig. 1, line b), which are comparable to those measured and reported [29,31,32] for the $Co(acac)_3$ precursor, 1591–1568 and 1535–1520 cm^{-1}. Similar results were obtained for the samples supported on 600-Al_2O_3. These adsorption bands and the methyl bands indicated the presence of acac-ligands on the $Co(acac)_x$ modified samples.

The band observed between 1296 and 1261 cm^{-1} for all samples in Fig. 1 (indicated with dotted lines, Al-acac and Co-acac) is sensitive to the central metal ion [34,35]. The values reported for $Co(acac)_2$ are from 1270 to 1255 cm^{-1} [30–33] and for $Co(acac)_3$ from 1284 to 1274 cm^{-1} [29,31,32]. In the IR spectra of the bulk precursors $Co(acac)_2$ and $Co(acac)_3$ this band was seen at 1261 and 1279 cm^{-1}, respectively. In the spectra of the supported samples the line was seen at 1263–1262 cm^{-1} (Fig. 1, lines a and b), i.e. the spectra of the supported $Co(acac)_3$ resembled more closely bulk $Co(acac)_2$ than $Co(acac)_3$. In the spectrum of the H(acac)/600–Al_2O_3 sample a band was seen at 1296 cm^{-1} (Fig. 1, line c). This corresponds to the values reported for $Al(acac)_3$, i.e. 1291–1280 cm^{-1} [29,31,33]. The band observed at 1292 cm^{-1} in the spectra of the modified samples for both precursors (Fig. 1, lines a and b), indicated the presence of $Al(acac)_x$ species [35]. This peak appeared for both precursors and both support pretreatment temperatures (600/875 °C) between 1292 and 1289 cm^{-1}.

3.2. Surface reactions

Surface reactions that should be considered for the cobalt acetylacetonate precursors $Co(acac)_2$ and $Co(acac)_3$ on alumina include; ligand exchange reaction with OH groups (1) (e.g. [23]). Dissociative adsorption on coordinatively unsaturated Al–O pairs (2) (e.g. [35,36]). Associative adsorption through hydrogen bonding, reaction (3a), or interaction with surface oxygen, reaction (3b). It has been proposed that a transformation of $Co(acac)_3$ to $Co(acac)_2$ would occur before chemisorption to the surface [23,37,38], reaction (4). In that case, the x in Eqs. (1)–(3) would equal 2. The H(acac) has been shown to react according to reaction (5) on alumina [35,39,40]. The shaded box denotes the support surface:

$$\square\text{–OH} + Co(acac)_x\,(g) \rightarrow H(acac)\,(g) + \square\text{–O–}Co(acac)_{x-1} \quad (1)$$

$$\square(AlO) + Co(acac)_x\,(g) \rightarrow \square Al(acac) + \square\text{–O–}Co(acac)_{x-1} \quad (2)$$

$$\square\text{–OH} + Co(acac)_x\,(g) \rightarrow Co(acac)_x\cdots HO\text{–}\square \quad (3a)$$

$$\square O + Co(acac)_x\,(g) \rightarrow \square O\cdots Co(acac)_x \quad (3b)$$

$$Co(acac)_3(sorg) \rightarrow Co(acac)_2(g) + \text{“acac”}(g) \quad (4)$$

$$\square(AlO) + H(acac)\,(g) \rightarrow \square Al(acac) + \square\text{–OH} \quad (5)$$

The DRIFT spectra showed that intact acac-ligands were present on the samples. The concentration of ligands can then be estimated from the amount of carbon on the samples. The carbon content on the $Co(acac)_2$-modified 600- and 875-Al_2O_3 (Table 1) corresponds to 2.6 and 2.8 ligands/nm^2, while for $Co(acac)_3$ the carbon amounts gives 3.2 and 3.5 ligands/nm^2, respectively. These concentrations equals to ligand/Co ratios of 1.1 and 1.5 for $Co(acac)_2$ and 1.9 and 2.3 for $Co(acac)_3$ (Table 1). The increase in ligand/Co ratio with pretreatment temperature indicated a change in the precursor support interaction.

Starting with $Co(acac)_2$, the ligand/Co ratio (Table 1) indicated that the main chemisorption mode is the ligand exchange reaction (1), which is the only reaction that gives a ratio of 1. The estimated ratios are slightly above one (1.1–1.5) and increase with pretreatment temperature, which indicates that a fraction of the precursor is adsorbed dissociatively (2) and/or that the ligand released in reaction (1) adsorbs dissociatively (5). The occurrence of a dissociative reaction on coordinatively unsaturated sites (either reaction (2) or (5)) was also indicated in the DRIFT spectra, which showed that Al-acac species were present on the surface (Fig. 1, lines a and c). The dissociative reactions should be more probable on alumina pretreated at 875 °C, i.e. with a higher concentration of coordinatively unsaturated sites and less OH groups. This is in line with the observed increase in the ligand/Co ratio.

The ligand/Co ratios obtained with $Co(acac)_3$ (1.9–2.3, Table 1) indicated that the main reaction would be the ligand exchange (1) also in this case, which would give a ligand/Co ratio of 2. However, assuming that $Co(acac)_3$ is transformed to $Co(acac)_2$ according to reaction (4) [23,24,37,38] the reaction mechanism, as well as the amount of cobalt and carbon, should be the same for both precursors. In order to obtain a ligand/Co ratio around 2, as observed, the precursor should mainly chemisorb either dissociatively (2) or associatively (3), which is in contradiction to what was found for the $Co(acac)_2$ modified samples. These results would not support the assumption that $Co(acac)_3$ transform to $Co(acac)_2$ before attaching to the surface, as has been suggested for $Co(acac)_3$ modified silica [23,24]. However, the released ‘ligand’ probably affects the carbon content and the number of reactive sites on alumina. Actually the acac-Co band in the DRIFT spectra of the $Co(acac)_3$ modified alumina resembles more closely that of adsorbed and bulk $Co(acac)_2$ than bulk $Co(acac)_3$. Similarly as for $Co(acac)_2$ the ligand/Co ratio increased with pretreatment temperature, again indicating increasing dissociative adsorption. Indications of Al-acac species were also seen in the DRIFT spectra (Fig. 1, lines b and c).

The OH group concentration on the 600- and 875-Al_2O_3 was 2 and 0.8 nm^{-2}, respectively. This corresponds to Co/OH ratios of 1.2 for $Co(acac)_2$ and 0.8 for $Co(acac)_3$ on alumina pretreated at 600 °C. On the 875-Al_2O_3 the ratios are 2.7 and 1.9, respectively. This indicates that the number of OH does not limit the surface reaction, at least not on the 875-Al_2O_3. The higher than unity Co/OH ratios indicate the occurrence of other interaction in addition to the ligand exchange reaction, e.g. dissociative adsorption, which supported the observations from the DRIFT spectra and the C/Co ratios. The observation that the cobalt content correlated with the

surface area of the support suggests that steric hindrance would be a limiting factor. Furthermore, the amount of cobalt per surface area of alumina was on average ca. 30% less with $Co(acac)_3$ than with $Co(acac)_2$. This could be due either to interference of the "acac"-ligand released in reaction (4), i.e. blocking of the surface sites, or the bulkier molecule, i.e. more ligands.

According to the results from the elemental analysis and the DRIFTS measurements the preferred mechanism for the interaction between $Co(acac)_2$ and alumina would be the ligand exchange (1) combined with some dissociative adsorption, reactions (2) and (5). These reactions would give a ligand/Co ratio between 1 and 2, as observed.

Based on the observations given above, two routes can be proposed for the interaction of $Co(acac)_3$ with alumina. The first reaction route, which is in accordance with what has been proposed for $Co(acac)_3$ on silica [23,24], is loss of a ligand (4) followed by similar reactions as given above for $Co(acac)_2$. The second route is a combination of mainly the ligand exchange reaction (1) and to some extent dissociative adsorption reactions (2) and (5). These routes would give ligand/Co ratios of 1–3 and 2–3, respectively, both in accordance with observations. It is not possible to conclude unambiguously from these results, which is the main mechanism. But based on previous results from $Co(acac)_3$ on silica [23,24] it seems probable that $Co(acac)_3$ transforms to $Co(acac)_2$ before reacting.

3.3. High loading catalysts

The high loading catalysts were prepared using $Co(acac)_2$ due to the possible interference of a ligand released when using $Co(acac)_3$. The cobalt content on the $Co(acac)_2$/875-Al_2O_3 catalysts was increased by repeating the precursor addition and calcination steps up to five times. During each repeated cycle (cycles 2–5) the cobalt content increased by ca. 1.7 wt.% Co on average (Table 1). The increase given in atoms per nm^2 is almost linear at ca. 1.5 Co/nm^2. The C/Co ratio of the third and fifth preparation cycle can be estimated based on the linear increase of cobalt loading and measured carbon content. The C/Co ratio of the last precursor addition step on the three- and five-cycle samples was 9.0 and 9.4, respectively. This corresponds to a ligand/Co ratio of 1.8 and 1.9 (Table 1), which indicates that both acac-ligands remained on the sample. The linear increase and the similar ligand/Co ratio suggested same type of interaction during the repeated preparation cycles. The ligand surface concentration was the same as for the one-cycle sample (around 2.8 ligands/nm^2, Table 1) but the ligand/Co ratio was higher than on the one-cycle sample. This indicates a change in the interaction compared to pure alumina. The fact that the ligand density still was the same can be explained by steric hindrance. The type of interaction during subsequent reaction cycles was not studied in greater detail, but the reaction sites were probably not limiting, e.g. new reaction sites were formed during the calcination. The cobalt packing density was very similar compared to what has been obtained on $Co(acac)_3$ modified silica [23,24]. The colour of the calcined catalysts went from bluish grey to black with increasing loading. The reduced (and reoxidised) samples went from bright blue to black. The blue colour of the low loading catalysts suggested the formation of cobalt aluminate.

3.4. Reducibility of the cobalt species

Calcination has been found to lower the reducibility of both $Co(acac)_3/SiO_2$ [12,14] and $Co(acac)_2/Al_2O_3$ catalysts [14]. The extent of reduction (550 °C/7 h) was found to increase with cobalt loading on both calcined and uncalcined $Co(acac)_2/Al_2O_3$ catalysts [14], which indicated decreasing interaction between the cobalt species and the support. The reducibility of the uncalcined catalysts was higher than of the calcined ones but the difference decreased at increasing loading [14].

Here the reducibility was studied over a larger temperature interval using O_2-titration and TPR. The extent of reduction as a function of the reduction temperature (450–650 °C) was measured for calcined and uncalcined $Co(acac)_2$ based samples containing 6.4 and 6.3 wt.% Co, respectively (Fig. 2). The fraction of metallic cobalt increased with the reduction temperature on both samples but it was clearly higher on the uncalcined sample. The degree of reduction of the calcined sample increased from 12 to 43% (450–600 °C), but the increase was marginal over the interval 550–600 °C (Fig. 2a). The degree of reduction of the uncalcined sample increased almost linearly from 44 to 85% (500–650 °C) (Fig. 2b). The lower reducibility of the calcined samples was probably due to formation of cobalt aluminate like species [1,8,14,15].

Reduction profiles as a function of temperature (TPR) were measured for both calcined (Fig. 3, i–iii) and uncalcined (Fig. 3, iv–vi) $Co(acac)_2$ samples with different cobalt contents. Practically no hydrogen consumption was observed for the calcined one-cycle sample (Fig. 3, i), indicating the presence a 'fully' dispersed cobalt oxide with a strong interaction with the alumina [2]. The species on the calcined catalysts with higher metal loading that reduced below 450 °C can be assumed to be Co_3O_4 reducing to CoO [16] and at higher temperatures further to Co. The species reducing above 600 °C are likely to be very strongly interacting CoO [16] and cobalt aluminate type compounds [15,18]. The peak below 200 °C might

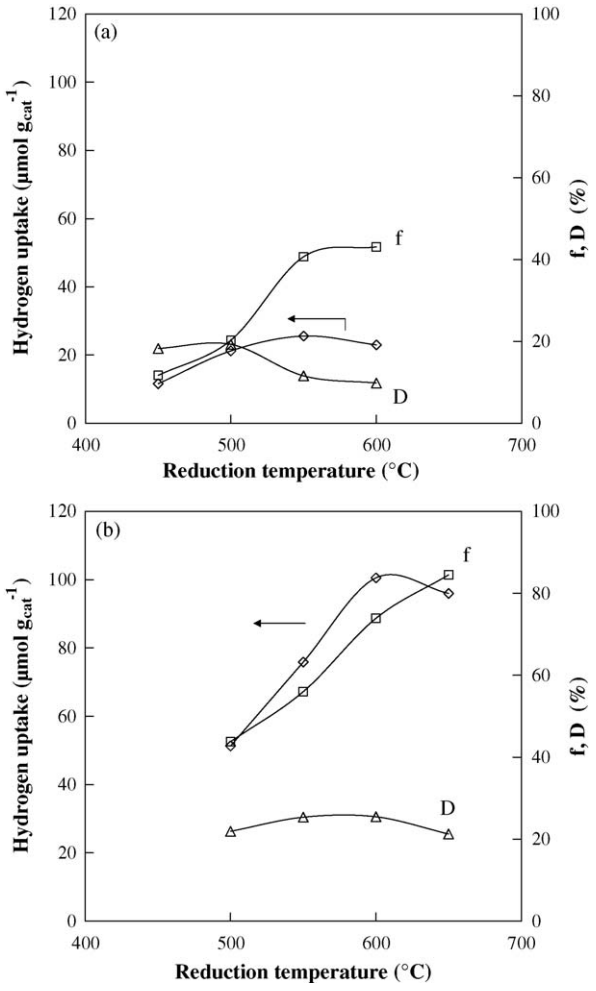

Fig. 2. Hydrogen uptake at 100 °C, degree of reduction and dispersion as a function of reduction temperature on $Co(acac)_2/Al_2O_3$ catalysts. (a) Calcined sample 6.4 wt.% Co. (b) Uncalcined sample 6.3 wt.% Co.

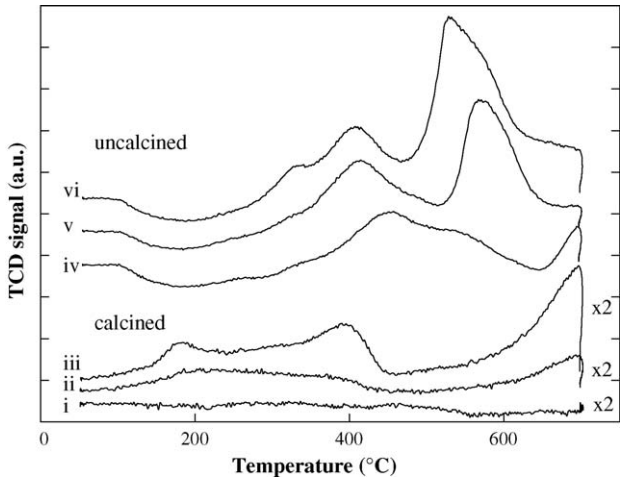

Fig. 3. TPR profiles of calcined and uncalcined $Co(acac)_2/Al_2O_3$ samples prepared by one-, three- and five-cycles (highest loading at the top).

be due to some residual carbonaceous material from the precursor since no cobalt species are expected to reduce at these temperatures.

The TPR profiles of the uncalcined samples do not directly represent hydrogen consumption, due to decomposition and reaction products from the surface species that affect the TCD signal. For example, during the TPR of the five-cycle sample (Fig. 3, vi) acetone was formed at 320–370 °C, methane at 530 °C and other hydrocarbon fragments (C_2 and C_3) at 320–450 °C. In addition, the cobalt oxide species from previous preparation cycles are reduced. It has been suggested that cobalt diffuses into the support during reduction [41], which could account for the high temperature reduction peak in the uncalcined one-cycle sample (Fig. 4, IV).

The calcination decreases the reducibility by forming a well dispersed oxide phase and cobalt aluminate species that are harder to reduce than the $Co(acac)_x$ species [14]. An analogous behaviour was seen on silica supported catalysts where cobalt silicate is formed [12,13]. Because the TCD signal in the TPR measurements is disturbed by acetone, water and hydrocarbons released from the acac-ligands it is difficult to follow the reduction of cobalt species. However, the O_2-titration measurements show that the uncalcined catalysts have higher degrees of reduction. Whether the $Co(acac)_x$ species actually functions as promoters, that facilitate reduction of cobalt species formed during the previous calcination steps [12], is more difficult to show. Optimisation of the calcination procedure is important, as has been shown for Ni/Al_2O_3 catalysts with $Ni(acac)_2$ as precursor [42]. Calcination at 250 °C improved the reducibility compared to direct reduction, while calcination at higher temperatures decreased the reducibility [42]. Furthermore, it has been shown that the use of nickel or cobalt ethylenediamine complexes in preparation of alumina supported catalysts can produce well dispersed reducible catalysts when no air calcination is performed [43,44]. Especially with nickel, the decomposition of the ethylenediamine ligands in an inert atmosphere caused autoreduction producing well dispersed metallic nickel particles [43]. The effect was not as strong with similar cobalt samples, which required further reduction with hydrogen [44]. In addition, the dispersion was less uniform for cobalt. Although the activation procedure is different it is possible that the decomposition products of the acetylacetonate ligands contribute to the reduction of cobalt also on the ALD samples.

Due to the difficulties in interpreting the TPR profiles of the fresh samples sequential reduction and oxidation treatment was applied before TPR. The effect of sequential reduction (550 °C) and

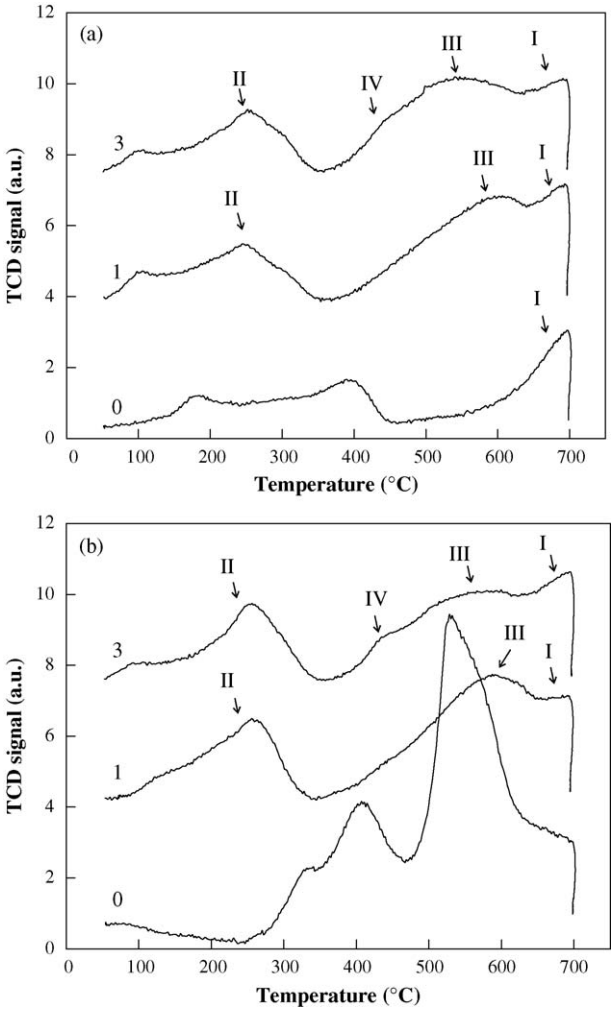

Fig. 4. TPR profiles of $Co(acac)_2/Al_2O_3$ catalysts (0) a fresh sample, (1) after one and (3) after three reduction/oxidation treatments. (a) Calcined sample 9.2 wt.% Co. (b) Uncalcined sample 9.8 wt.% Co.

oxidation (450 °C) treatment was studied for a calcined and an uncalcined five-cycle $Co(acac)_2/Al_2O_3$ sample (Fig. 4). The most noticeable change was seen after the first reduction/oxidation cycle, additional treatment had only a minor effect on the TPR profiles. The calcined and the uncalcined sample showed similar hydrogen consumption after one or more reduction/oxidation cycles. All samples showed species reduction above 600 °C (Fig. 4, I), the peak is especially prominent in the fresh calcined sample, probably aluminate type species [15]. The hydrogen consumption below 350 °C (Fig. 4, II) can be ascribed the reduction of Co_3O_4 to CoO [15,16]. With subsequent reduction of CoO to Co above 400 °C (Fig. 4, III), this broad feature between 400 and 650 °C with a maximum at about 570 °C appeared after one reduction/oxidation cycle. This indicates formation of more reducible cobalt species due to the reduction/oxidation treatment. After further treatment, a shoulder appeared at about 440 °C (Fig. 4, IV), probably due to sintering, i.e. formation of larger particles with less interaction with the support. The low temperature peak around 100 °C could not be ascribed to any cobalt species.

3.5. Dispersion of cobalt

The dispersion of cobalt on the samples was estimated based on the total hydrogen uptake at 100 °C. The one-cycle samples, both calcined and uncalcined, showed a very low surface area of

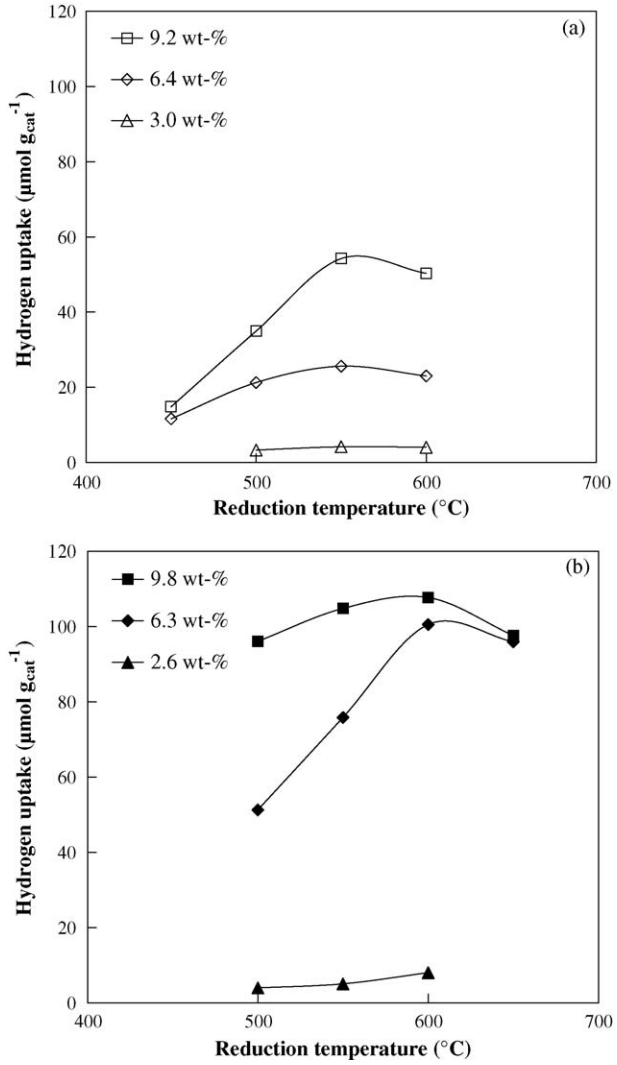

Fig. 5. Hydrogen uptake at 100 °C from static volumetric measurements, as a function of reduction temperature, on $Co(acac)_2/Al_2O_3$ catalysts. (a) Calcined samples (open symbols). (b) Uncalcined samples (filled symbols).

metallic cobalt, which was expected due to the low reducibility. The hydrogen uptake increased with loading on both calcined and uncalcined samples, but the uptake on the uncalcined samples was on a significantly higher level (Fig. 5). A maximum was observed in the hydrogen uptake as a function of reduction temperature at 550 °C on the calcined $Co(acac)_2$ based catalysts (Fig. 5a) and at 600 °C on the uncalcined ones (Fig. 5b). However, the highest dispersion on the three-cycle samples were obtained after reduction at about 450–500 °C on the calcined sample and at about 550–600 °C on the uncalcined sample (Fig. 2). The dispersions shown in Fig. 2 are corrected with the degrees of reduction. The particle size estimated using the hydrogen uptake on the three- and five-cycle samples were about 8 nm on the calcined and 4–5 nm on the uncalcined samples. The small particle sizes are in line with the observed strong interaction.

In addition to the H_2 chemisorption the CO chemisorption capacity was measured on both reduced and calcined samples. The interpretation of the CO chemisorption measurements are not as straightforward as for H_2, the stoichiometry varies depending on the types of adsorbed CO species (linear, bridged and polycarbonyls) [26,45]. Furthermore, the CO molecule also adsorb on unreduced cobalt species [46]. As for the H_2 chemisorption the CO chemisorption capacity on the reduced $Co(acac)_2$ based catalysts generally increased with loading and it was higher on the uncalcined samples than on the calcined ones (Table 2). The ratio of the total CO at 30 °C and total H_2-chemisorption at 100 °C ($CO_{t,30°C}/H_{t,100°C}$) decreased with increasing loading (Table 2). Adsorption of CO on non-metallic species was probably the reason for the observed high total CO chemisorption capacity at low loading. However, the chemisorption of CO on non-metallic species is very reversible, which was seen also here on calcined unreduced samples, where only about 30% of the CO was irreversibly adsorbed. The CO chemisorption on the reduced low loading samples is very reversible due the large fraction of cobalt that is present as non-metallic species. The fraction of irreversibly chemisorbed CO on the reduced samples increased with loading, i.e. with the surface area of metallic cobalt. The ratio of irreversibly chemisorbed CO and total hydrogen ($CO_{i,30°C}/H_{t,100°C}$) was equal to or below one (Table 2) with no clear correlation with dispersion.

Looking at the increase in degree of reduction and the increase in hydrogen uptake i.e. metal surface area, it seems that the uncalcined samples are less susceptible to sintering than the calcined ones over the studied temperature range. The dispersion starts to decrease above 500 °C on the calcined sample (Fig. 2a) and above 550–600 °C on the uncalcined sample (Fig. 2b). The thermal stability of the samples was further studied by looking at the changes in metallic surface area during reduction (550 °C) and oxidation cycles (450 °C) (Fig. 6). The relative decrease in the hydrogen uptake, i.e. in the metal surface area, during the reduction/oxidation cycles was smaller on calcined samples. However, the hydrogen uptake on the uncalcined samples remained higher than on the calcined ones. The ALD catalysts seem to maintain the cobalt surface area despite repeated reduction/oxidation cycles. This was also indicated in the TPR profiles, which showed only minor changes in the supported species. Highly dispersed thermally stable catalysts were obtained, however the reducibility could probably benefit from the addition of a promoter [1,2,5,15,16,19,20].

Table 2
Chemisorption of CO on $Co(acac)_2$ based catalysts (t, total and i, irreversible).

Cycles	Co (wt.%)	T_{red} (°C)	$CO_{t,30°C}$ (μmol g_{cat}^{-1})	$CO_{i,30°C}$ (%)	$CO_{t,30°C}/H_{t,100°C}$	$CO_{i,30°C}/H_{t,100°C}$
$Co(acac)_2$ calcined						
1	3.0	550	58.8	6.6	7.1	0.47
3	6.4	550	127	41	2.5	1.0
5	9.2	550	142	47	1.3	0.62
1	3.0	calc.	57.6	28		
3	6.4	calc.	89.5	30		
5	9.2	calc.	90.0	31		
$Co(acac)_2$ uncalcined						
1	2.6	550	59.2	15	5.8	0.90
3	6.3	550	220	67	1.5	0.97
5	9.8	550	210	67	1.0	0.67

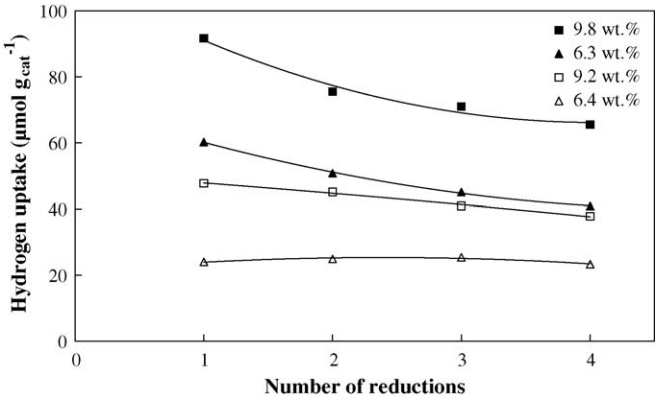

Fig. 6. Hydrogen uptake at 100 °C from static volumetric measurements, as a function of reduction/oxidation cycles, on calcined (open symbols) and uncalcined (filled symbols) $Co(acac)_2/Al_2O_3$ catalysts. The *x*-axis indicates number of reductions.

Table 3
Gas phase hydrogenation of toluene on Co/Al_2O_3. Hydrogen uptake, average cobalt particle size, maximum reaction rate and turn over frequency is shown.

Cycles	Co (wt.%)	T_{red} (°C)	H_2 uptake (μmol g_{cat}^{-1})	d (nm)	r_{max} (μmol g_{cat}^{-1})	TOF_{max} (s^{-1})
3	6.3	550	75.9	3.8	5.8	0.038
5	9.8	550	105	5.2	6.7	0.032
3	6.4	550	25.6	8.3	2.4	0.046

3.6. Toluene hydrogenation

Gas phase hydrogenation of toluene (H_2:Tol/12:1) was studied between 30 and 150 °C in a transient mode. A maximum was observed in the reaction rate at 100 ± 5 °C. A maximum in the reaction rate as a function of temperature is typical for hydrogenation of aromatic compounds on metals, e.g. Ni [47,48] and Co [14,49]. We have previously found the maximum at about 100–110 °C on cobalt in similar conditions to be independent of support and cobalt loading (silica or alumina) [14]. The reaction rate maximum is probably due to a decrease in surface coverage of some surface species, either hydrogen [14,47], aromatic [48] or both, with increasing temperature. A decrease in the surface coverage of hydrogen seems probable based on previous results. It has been shown by temperature programmed desorption (TPD) that the hydrogen desorption rate on cobalt increases significantly above 100 °C [14].

Although the hydrogenation of aromatics is generally considered a structure insensitive reaction, as is typical for transition metal catalyzed hydrocarbon hydrogenation reactions [50], there are results suggesting a particle size effect at low reaction temperatures (25–120 °C) for some metals (Ni, Rh, Pd and Pt) [51]. A possible effect of the particle size was studied using Co/Al_2O_3 samples with different average cobalt particle sizes, 3.8–8.3 nm (Table 3). The maximum reaction rate is given in Table 3. The reaction rate per surface cobalt atom, or turn over frequency (TOF), was calculated using the total hydrogen uptake (Table 3). The maximum reaction rate correlated with the hydrogen uptake, i.e. cobalt surface area. No clear correlation between the TOF values and the average particle size was observed.

4. Conclusions

Alumina supported cobalt catalysts were prepared by atomic layer deposition (ALD) from cobalt acetylacetonates ($Co(acac)_2$, $Co(acac)_3$). The interaction of the cobalt acetylacetonate precursors with alumina pretreated at 600 or 875 °C was proposed to occur both via a ligand exchange reaction with OH groups and via dissociative adsorption on coordinatively unsaturated sites. The cobalt content added during one reaction cycle correlated with the surface area of the support, i.e. steric hindrance limited the amount of precursor.

Higher loading catalysts were prepared by repeating precursor adsorption ($Co(acac)_2$) and calcination steps. However, calcination with air at 450 °C decreased the reducibility of the $Co(acac)_2$ based catalyst. Cobalt oxide species interacting strongly with the alumina support was formed during calcination. Samples were also prepared where the last calcination step was omitted, i.e. uncalcined catalysts.

The highest cobalt surface area was obtained on the uncalcined $Co(acac)_2$ samples, i.e. where the precursor was reductively decomposed. Strong interaction between the cobalt species and the support was observed from TPR studies, especially at low cobalt loading. The degree of reduction increased with cobalt loading, i.e. with decreasing interaction. Also the dispersion decreased on the $Co(acac)_2$ based catalysts due to calcination. However, both the calcined and uncalcined samples were well dispersed with cobalt particle sizes of ca. 8 and 4–5 nm, respectively, for loadings of 6–10 wt.% Co. The catalytic activity for toluene hydrogenation correlated with the cobalt surface area.

Acknowledgements

The Academy of Finland and the Nordic Energy Program, Division of Petroleum Technology are acknowledged for financial support. The Technical Research Centre of Finland (VTT) and the Centre for Chemical Analysis at the Helsinki University of Technology are thanked for cobalt determinations. Ms. Kati Vilonen is thanked for performing a part of the experimental work.

References

[1] G. Jacobs, T.K. Das, Y. Zhang, J. Li, G. Racoillet, B.H. Davis, Appl. Catal. A 233 (2002) 263–281.
[2] S.L. Soled, E. Iglesia, R.A. Fiato, J.E. Baumgartner, H. Vroman, S. Miseo, Top. Catal. 26 (2003) 101–109.
[3] G.L. Bezemer, J.H. Bitter, H.P.C.E. Kuipers, H. Oosterbeek, J.E. Holewijn, X. Xu, F. Kapteijn, A. Jos van Dillen, K.P. de Jong, J. Am. Chem. Soc. 128 (2006) 3956–3964.
[4] D. Schanke, A.M. Hilmen, E. Bergene, K. Kinnari, E. Rytter, E. Ådanes, A. Holmen, Energy Fuels 10 (1996) 867–872.
[5] A.M. Hilmen, D. Schanke, K.F. Hanssen, A. Holmen, Appl. Catal. A 186 (1999) 169–188.
[6] G. Jacobs, P.M. Patterson, T.K. Das, M. Luo, B.H. Davis, Appl. Catal. A (2004) 65–76.
[7] A. Lapidus, V. Krylova, V. Kazanskii, A. Borovkov, J. Zaitsev, A. Rathousky, M. Zukal, Jancálková, Appl. Catal. 73 (1991) 65–82.
[8] M. Voß, D. Borgmann, G. Wedler, J. Catal. 212 (2002) 10–21.
[9] J.M. Jabłoński, M. Wolcyrz, L. Krajczyk, J. Catal. 173 (1998) 530–534.
[10] B. Ernst, S. Libs, P. Chaumette, A. Kiennemann, Appl. Catal. A 186 (1999) 145–168.
[11] D. Potoczna-Petru, L. Krajczyk, Catal. Lett. 87 (2003) 51–56.
[12] L.B. Backman, A. Rautiainen, A.O.I. Krause, M. Lindblad, Catal. Today 43 (1998) 11–19.
[13] L.B. Backman, A. Rautiainen, M. Lindblad, O. Jylhä, A.O.I. Krause, Appl. Catal. A 208 (2001) 223–234.
[14] L.B. Backman, A. Rautiainen, M. Lindblad, A.O.I. Krause, Appl. Catal. A 191 (2000) 55–68.
[15] B. Jongsomjit, J. Panpranot, J.G. Goodwin Jr., J. Catal. 204 (2001) 98–109.
[16] G. Jacobs, Y. Ji, B.H. Davis, D. Cronauer, A.J. Kropf, C.L. Marshall, Appl. Catal. A 333 (2007) 177–191.
[17] D.I. Enache, B. Rebours, M. Roy-Auberger, R. Revel, J. Catal. 205 (2002) 346–353.
[18] B. Jongsomjit, J.G. Goodwin Jr., Catal. Today 77 (2002) 191–204.
[19] D.G. Moen, B.S. Nicholson, P.L. Clausen, A. Hansen, G. Molenbroek, Steffensen, Chem. Mater. 9 (1997) 1241–1247.
[20] W. Chu, P.A. Chernavskii, L. Gegembre, G.A. Pankina, P. Fongarland, A.Y. Khodakov, J. Catal. 252 (2007) 215–230.
[21] J.W. Bae, Y.-J. Lee, J.-Y. Park, K.-W. Jun, Energy Fuels 22 (2008) 2885–2891.
[22] R.L. Puurunen, J. Appl. Phys. 97 (2005), 121301-121301-52.
[23] Rautiainen, M. Lindblad, L.B. Backman, R.L. Puurunen, Phys. Chem. Chem. Phys. 4 (2001) 2466–2472.
[24] R.L. Puurunen, T.A. Zeelie, A.O.I. Krause, Catal. Lett. (2002) 27–32.
[25] J. Xiong, Ø. Borg, E.A. Blekkan, A. Holmen, Catal. Commun. 9 (2008) 2327–2330.
[26] R.C. Reuel, C.H. Bartholomew, J. Catal. 85 (1984) 63–77.

[27] M.K. Niemelä, L. Backman, A.O.I. Krause, T. Vaara, Appl. Catal. 156 (1997) 319–334.
[28] A. Kytökivi, M. Lindblad, A. Root, J. Chem. Soc., Faraday Trans. 191 (1995) 941–948.
[29] K. Nakamoto, P.J. McCarthy, A. Ruby, A.E. Martell, J. Am. Chem. Soc. 83 (1961) 1066–1069.
[30] K. Nakamoto, P.J. McCarthy, A.E. Martell, J. Am. Chem. Soc. 83 (1961) 1272–1276.
[31] J.P. Dismukes, L.H. Jones, J.C. Bailar Jr., J. Phys. Chem. 65 (1961) 792–795.
[32] J.G. Grasselli, W.M. Ritchey, A. Hiraki (Eds.), 2nd edn., Atlas of Spectral Data and Physical Constants for Organic Compounds, vol. IV, CRC Press, Cleveland, OH, 1975, pp. 26–28.
[33] L.O. Nindakova, F.K. Shmidt, V.V. Saraev, B.A. Shainyan, N.N. Chipanina, V.A. Umanets, L.N. Belonogova, D-S.D. Toryashinova, Kinet. Catal. 47 (2006) 54–63.
[34] M. Mikami, I. Nakagawa, T. Shimanouchi, Spectrochim. Acta 23A (1967) 1037–1053.
[35] J.A.R. van Veen, G. Jonkers, W.H.J. Hesselink, Chem. Soc., Faraday Trans. 185 (1989) 389–413.
[36] M. Lindblad, L.P. Lindfors, T. Suntola, Catal. Lett. 27 (1994) 323–336.
[37] G. Beech, R.M. Lintonbon, Thermochim. Acta 3 (1971) 97–105.
[38] I. Yoshida, H. Kobayashi, K. Ueno, Bull. Chem. Soc. Jpn. 47 (1974) 2203–2207.
[39] A. Kytökivi, A. Rautiainen, A. Root, J. Chem. Soc., Faraday Trans. 93 (1997) 4079–4084.
[40] I.V. Babich, Yu.V. Plyuto, A.D. Van Langeveld, J.A. Moulijn, Appl. Surf. Sci. 115 (1997) 267–272.
[41] A.M. Hilmen, D. Schanke, A. Holmen, Catal. Lett. 38 (1996) 143–147.
[42] R. Molina, G. Poncelet, J. Catal. 199 (2001) 162–170.
[43] F. Négrier, E. Marceau, M. Che, D. De Caro, C. R. Chim. 6 (2003) 231–240.
[44] F. Dumond, E. Marceau, M. Che, J. Phys. Chem. C 111 (2007) 4780–4789.
[45] G. Kadinov, Ch. Bonev, S. Todorova, A. Palazov, J. Chem. Soc., Faraday Trans. 94 (1998) 3027–3031.
[46] D. Pope, D.S. Walker, L. Whalley, R.L. Moss, J. Catal. 31 (1973) 335–345.
[47] L.P. Lindfors, T. Salmi, S. Smeds, Chem. Eng. Sci. 48 (1993) 3813–3828.
[48] M.A. Keane, J. Catal. 166 (1997) 347–355.
[49] W.F. Taylor, H.K. Stafflin, J. Phys. Chem. 71 (1967) 3314–3319.
[50] R.A. Van Santen, Acc. Chem. Res. 42 (2009) 57–66.
[51] M. Che, C.O. Bennett, Adv. Catal. 36 (1989) 55–172.